Cell Reports

Report

Injection of Antibodies against Immunodominant Epitopes Tunes Germinal Centers to Generate Broadly Neutralizing Antibodies

Graphical Abstract

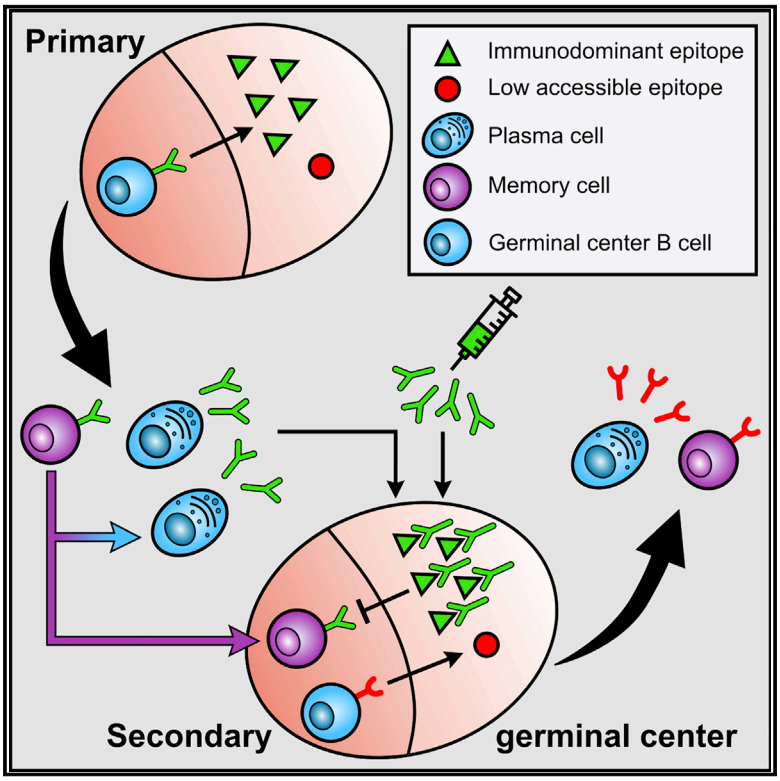

Authors

Michael Meyer-Hermann

Correspondence

mmh@theoretical-biology.de

In Brief

Antibodies specific for low-accessible pathogen epitopes are crucial for the control of life-threatening infections. Meyer-Hermann shows with computer simulations that memory-derived antibodies mask immunodominant epitopes, suppress participation of memory B cells in germinal centers, and promote affinity maturation to less-accessible epitopes. Vaccination with antibodies can induce the same effect.

Highlights

- Injected or pre-exisiting antibodies mask immunodominant epitopes in germinal centers
- Epitope masking can shift the focus of germinal centers to less-accessible epitopes
- Memory B cells are less competitive in germinal centers with masked epitopes
- Memory-derived antibodies promote natural affinity maturation to other epitopes

Meyer-Hermann, 2019, Cell Reports *29*, 1066–1073
October 29, 2019
https://doi.org/10.1016/j.celrep.2019.09.058

CellPress

OPEN ACCESS
CellPress

Cell Reports
Report

Injection of Antibodies against Immunodominant Epitopes Tunes Germinal Centers to Generate Broadly Neutralizing Antibodies

Michael Meyer-Hermann[1,2,3,4,5,*]
[1]Department of Systems Immunology and Braunschweig Integrated Centre of Systems Biology, Helmholtz Centre for Infection Research, Braunschweig, Germany
[2]Centre for Individualized Infection Medicine (CIIM), Hannover, Germany
[3]Institute for Biochemistry, Biotechnology and Bioinformatics, Technische Universität Braunschweig, Braunschweig, Germany
[4]Cluster of Excellence RESIST (EXC 2155), Hannover Medical School, Carl-Neuberg-Straβe 1, 30625 Hannover, Germany
[5]Lead Contact
*Correspondence: mmh@theoretical-biology.de
https://doi.org/10.1016/j.celrep.2019.09.058

SUMMARY

Broadly neutralizing antibodies are crucial for the control of many life-threatening viral infections like HIV, influenza, or hepatitis. Their induction is a prime goal in vaccine research. Using computer simulations, we identify strategies to promote the generation of broadly neutralizing antibodies in natural germinal center (GC) reactions. The simulations predict a feedback loop based on antibodies and memory B cells from previous GC reactions that promotes GCs to focus on new epitopes. Memory-derived or injected antibodies specific for immunodominant epitopes control epitope availability, suppress the participation of memory B cells in the GC reaction, and allow for the evolution of other B cells to affinity mature for hidden or rare epitopes. This defines a natural selection mechanism for GC B cells to concentrate on new epitopes rather than refine affinity to already-covered epitopes. This principle can be used for the design and testing of future therapies and vaccination protocols.

INTRODUCTION

In vaccine research, major efforts aim at inducing the generation of broadly neutralizing antibodies (bnAbs) against viral epitopes in influenza, hepatitis C virus, or HIV (Corti et al., 2017; Murira et al., 2016; Pegu et al., 2017). bnAbs are either cross-reactive against different epitopes in a hypervariable region or target a conserved region of the viral antigen (Mascola and Haynes, 2013). They occasionally develop in patients and target different epitopes of the viral antigen (Scheid et al., 2009). It was shown for HIV that one may design bnAbs in mice by sequential immunization with a slightly modified antigen (Escolano et al., 2016). In this way, a sequence of multiple germinal center (GC) reactions is induced, which targets an antigen-epitope converging to the desired bnAb in small steps. Thereby, the repertoire and frequency of GC precursor B cells plays an important role for the chance of developing bnAbs (Abbott et al., 2018; Havenar-Daughton et al., 2018). There is currently no strategy of how to foster the generation of bnAbs in single GC reactions, and vaccination research so far failed to induce bnAbs by immunization (Schiffner et al., 2013). For example, vaccination against influenza is often not successful because the antibodies target highly variable epitopes on the viral surface molecule hemagglutinin (Smith et al., 2004), which is only effective when the viral strain matches the targets (Tricco et al., 2013).

In order to avoid antigenic drift and viral escape, it may be more advantageous to develop antibodies targeting the conserved regions of the virus. Conserved regions are essential for virus functionality, such that viral escape by mutations in these regions would induce a major inhibition in viral entry or replication. Indeed, in the case of HIV, bnAbs target epitopes in the conserved region of the antigen (Kwong and Mascola, 2018). However, these conserved targets are difficult to access by antibodies because the variable regions act as a shield and hide the conserved regions (Helle et al., 2011). In GCs, the native antigen is presented on follicular dendritic cells (FDCs) such that, in principle, it might be possible to find affinity maturation for conserved epitopes, which explains why bnAbs are occasionally found in humans. However, shielding by the immunodominant variable region makes interactions of B cell receptors with conserved epitopes rare and prevents the development of high-affinity antibodies in most cases (Havenar-Daughton et al., 2017).

There is no existing strategy of how to tune GC reactions to focus on one or the other epitope. Mathematical modeling and computer simulations have been used before to analyze the generation of high-affinity and cross-reactive antibodies (De Boer and Perelson, 2017; Meyer-Hermann et al., 2012; Oprea and Perelson, 1997; Wang et al., 2015). Mathematical models validated by a large set of experimental data are suitable instruments to predict possible ways of modulating the focus of GC reactions. In an elegant study, it was found that pre-existing antibodies might prevent the generation of bnAbs (Zarnitsyna et al., 2016). Indeed, GC-derived or injected antibodies enter the GC reaction and bind to the antigen presented on FDCs (Zhang et al., 2013). They compete with the B cell receptor for binding the target epitope and prevent

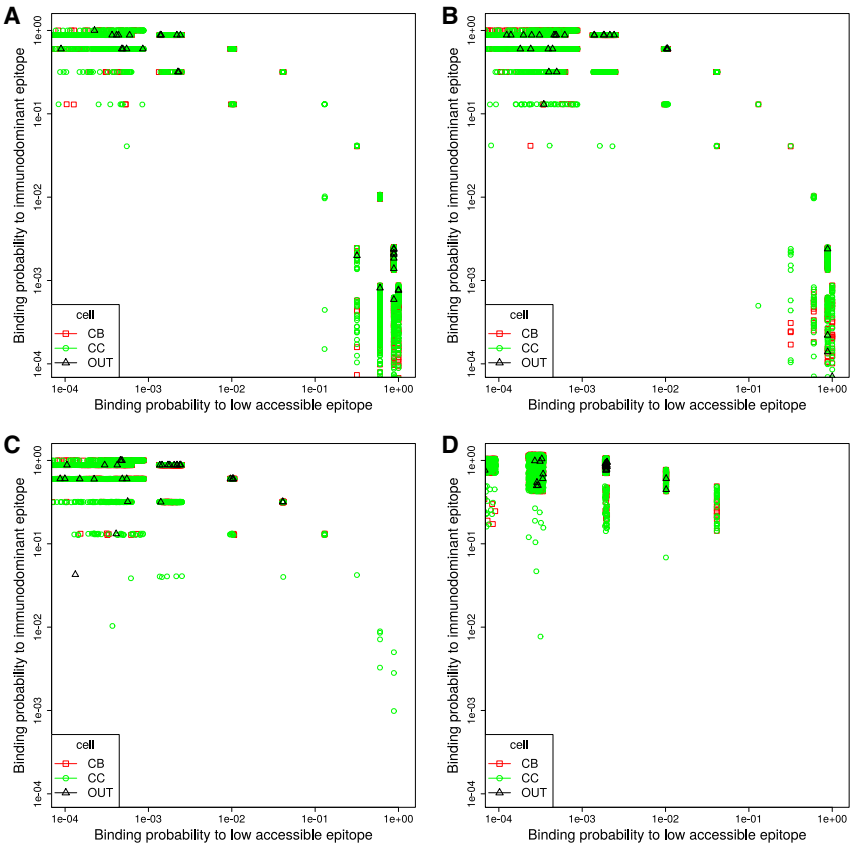

Figure 1. Affinity Maturation Requires a Minimum Accessibility of the Target Epitope

(A–D) *In silico* GC affinity maturation at day 11 post GC onset under the presence of two epitopes with different levels of relative accessibility: 50:50 (A), 30:70 (B), 10:90 (C), and 3:97 (D). Both epitopes are unrelated to each other (at a distance of 8 mutations). The color code distinguishes dark zone (red squares, CB) and light zone (green circles, CC) GC-B cells and GC output cells (black triangles, OUT). Representative single simulation for each condition.

B cell selection in a concentration- and affinity-dependent way. Even though the presence of immune complexes on FDCs seems dispensable for affinity maturation (Hannum et al., 2000), the presence of high-affinity antibodies can strongly inhibit or shut down the GC reaction (Zhang et al., 2013). Here, the impact of antibodies specific for immunodominant viral epitopes on affinity maturation of antibodies specific for hardly accessible epitopes is investigated with computer simulations.

RESULTS

A GC simulation platform was developed that enables the analysis of affinity maturation in the presence of multiple antigen epitopes. Starting from a state-of-the-art GC simulation software (Meyer-Hermann et al., 2012; Meyer-Hermann, 2014; Papa et al., 2017), the impact of antibodies specific for one epitope onto affinity maturation to other epitopes is investigated. Cell objects are defined in a three-dimensional space; antigen epitopes and antibodies are represented in an abstract affinity space (Perelson and Oster, 1979), which heuristically reflects the physical binding properties of antibody and antigen. This implies that the results of this paper are conceptual and that a quantitative application to a particular antigen would have to rely on data relating mutations and affinity specific for this antigen. Cells can move, interact, differentiate, divide, mutate, and die according to generally accepted knowledge about mechanisms of B cell evolution (Victora and Nussenzweig, 2012). Cellular objects include FDCs, dividing B cells, B cells in the state of apoptosis versus selection, and T follicular helper cells (Tfhs). B cells can sensitize and desensitize for chemokines specific for both GC zones (Figge et al., 2008). Cell motility and the frequency of migration between the zones in the model (Binder and Meyer-Hermann, 2016) are in accordance with two-photon experiments (Allen et al., 2007; Hauser et al., 2007; Schwickert et al., 2007; Victora et al., 2010). The complex and experimentally validated simulation was consciously chosen to allow for the identification of the relevant mechanisms that dominate the impact of antibodies onto the immune response to different epitopes.

B cells need to collect antigen from multiple contacts with FDCs for survival. Each antigen epitope is presented on each FDC site at different fractions in order to distinguish high- and low-accessible epitopes. It is assumed that the probability for a B cell to bind an epitope depends on the affinity of the B cell receptor for the epitope and the accessibility of the epitope. Thereby, the B cells attempt to bind the epitope of highest affinity (default) or of highest accessibility. If the latter option was used, this is explicitly mentioned. Every uptake event reduces the amount of antigen presented on FDCs. Optionally, antibodies, either injected or generated by GC-derived plasma cells, compete with B cells for binding the epitopes following classical chemical kinetics equations. They are degraded with a half-life of 2 weeks. The antibodies reduce the accessibility of the respective epitopes, and by this reduce the probability for a B cell to bind the antigen.

Selection of B cells for re-entering cell cycle or final differentiation to plasma or memory cells requires Tfh signaling (Meyer-Hermann et al., 2006; Victora et al., 2010). Tfh cells, in contrast to GC B cells, are not clonally restricted and migrate between different GCs (Shulman et al., 2013). It is, therefore, assumed in the model that Tfh cells for immunodominant or hidden epitopes are present. A threshold Tfh signal has to be achieved in B cells by the integration of signals from multiple

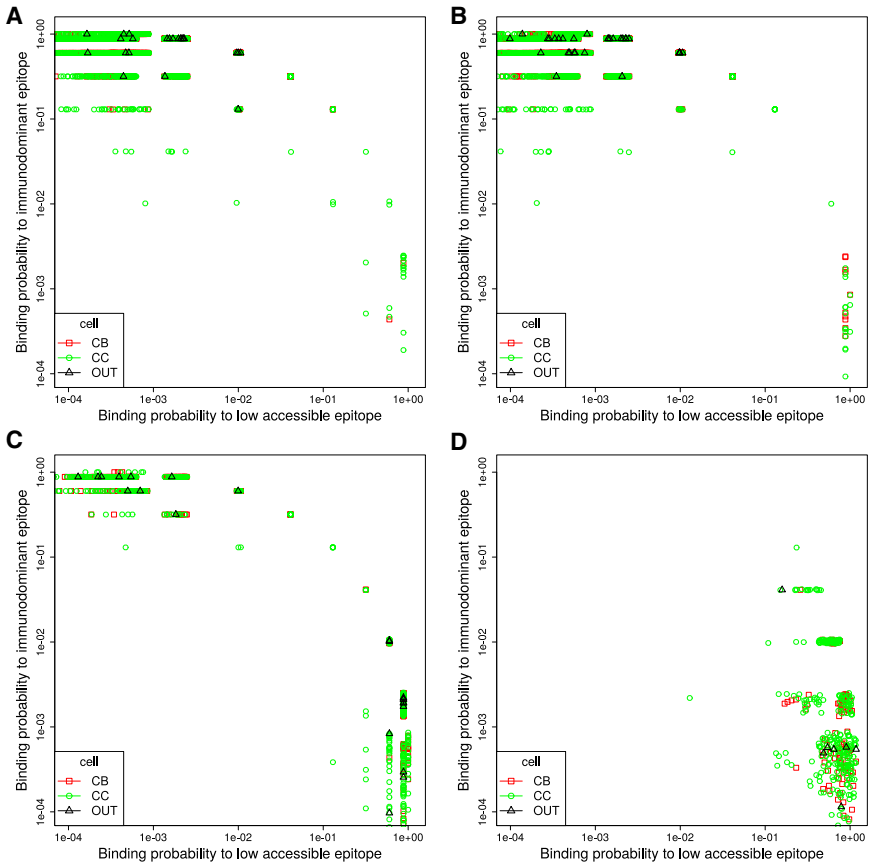

Figure 2. Affinity Maturation to Two Epitopes in Presence of Specific Antibodies

In silico GC affinity maturation to two epitopes with 10:90 accessibility at day 11 post GC onset under the presence of specific antibodies against the immunodominant epitope (vertical axis).

(A) Antibodies are derived from the GC reaction itself.

(B–D) Antibodies are injected at day 3 post GC onset with concentrations of 0.5 (B), 5 (C), and 50 (D) nMol, respectively. Both epitopes are unrelated to each other (at a distance of 8 mutations). The color code distinguishes dark zone (red squares, CB) and light zone (green circles, CC) GC-B cells and GC output cells (black triangles, OUT).

Representative single simulation for each condition.

T-B-interactions of 6 min each (Papa et al., 2017; Wang et al., 2016). Tfh signaling intensity increases with the amount of collected antigen, i.e., with the density of peptide major histocompatibility complex (pMHC) presentation by B cells. Selected B cells return to the dark zone for further division and mutation, where the number of divisions depends on the amount of collected antigen (Gitlin et al., 2014; Meyer-Hermann et al., 2012). For a more detailed description of the GC simulation, please refer to the Supplementary Material.

Some characteristics of the reference simulation are summarized in Figure S1. With a single antigen-epitope in the GC reaction, one can find a diversification of B cell receptors at day 3, which is then confined to higher affinity to the presented epitope over the time of the reaction (Figures S1D–S1F). In the presence of a second unrelated epitope with the same frequency, the GC gives rise to B cells specific to each epitope (Figure 1A). Thus, a single GC environment can give rise to two widely independent affinity maturation processes to two different epitopes.

A hardly accessible epitope in the conserved region is mimicked *in silico* by a reduced frequency of its presentation on FDC sites. In the simulations, GC affinity maturation concentrates on the immunodominant epitope (Figures 1B–1D). When the probability of catching the low-accessible epitope drops to 10% or lower, no affinity maturation against this epitope is observed (Figures 1C and 1D). This shows that under the presence of an immunodominant epitope, affinity maturation to other epitopes with lower accessibility is suppressed.

The *in silico* GCs in Figure 1 ignore the antibodies generated by the GC reaction output. However, it was previously shown that not only do the products of the GC reaction, antibody-forming plasma cells, efficiently produce antibodies but also that these antibodies distribute over the whole organism. In particular, they enter the GC reactions from which they are derived and compete with GC B cells for binding antigen on FDCs (Zhang et al., 2013). In order to analyze the effect of these competitive antibodies, it is assumed that the antibody concentration found in each *in silico* GC stems from the sum of the output cells of all GC reactions in the organism and is diluted over the whole blood and lymph system. A corresponding reference simulation is characterized in Figure S2. At the accessibility ratio of 10:90 (Figure 1), the feedback of antibodies induces affinity maturation for the low-accessible epitope (Figure 2A). This happens in a late phase of the GC reactions when affinity maturation against the immunodominant epitope is completed and a sufficient specific antibody was generated to mask the immunodominant epitope in the GC and increase the likelihood of binding the second epitope. However, the concentration of produced high-affinity antibodies (dissociation constant K_D <2 nMol) is a factor of 0.025 smaller compared to normal GC output and, thus, likely insufficient for a protective immune response. This holds true irrespective of the chosen GC exit model (Figure S4). Continuation of the GC simulation for another 3 weeks reveals that the GC response against the low-accessible epitope does not take off again (data not shown) because the selection probability is so low that the GC B cell population reaches zero *in silico* before the immunodominant epitope is suppressed by antibodies. These results show that the presence of antibodies specific for the immunodominant epitopes influences affinity maturation for

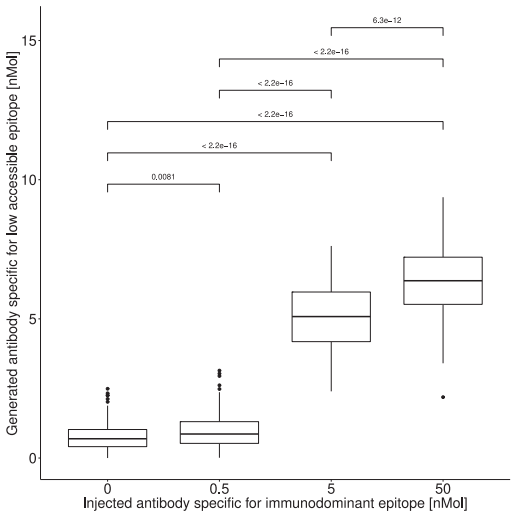

Figure 3. Antibody Injection Induces More Antibodies against Low-Accessible Epitopes

The total amount of antibodies specific (dissociation constant K_D, <2 nMol) for the low-accessible epitope generated by a single *in silico* GC reaction at day 21 post GC onset (i.e., at the end of the reaction) without (left) and with different concentrations (0.5, 5, and 50 nMol) of injected antibodies specific for the immunodominant epitope. Boxplots of 120 simulations for each condition. p values were calculated with R and the ggpubr package using the Mann-Whitney-Wilcoxon test and adjusted for multiple testing using the Benjamini-Hochberg approach.

low-accessible epitopes but that the naturally produced antibodies hardly induce a full-scale response against those.

The feedback of antibodies generated by the GC output itself might be too late to shift the focus of the GC reaction to a different epitope. Injection of high-affinity antibodies specific for the immunodominant epitope at the beginning of the *in silico* GC reaction can stabilize the generation of high-affinity output cells specific for the low-accessible epitope (Figures 2B–2D and 4C). This effect is also reflected in the total antibody generated against the low-accessible epitope (Figure 3) and is dependent on the concentration of the injected antibody against the immunodominant epitope. For low concentrations, the injected antibody increases the relative accessibility of the low-accessible epitope. Affinity maturation against both epitopes co-exist. At intermediate antibody concentrations, the affinity maturation for the low-accessible epitope becomes dominant. When the generated antibodies cover the low-accessible epitope, a second wave of affinity maturation against the immunodominant epitope is deliberated. At high concentrations of injected antibody, affinity maturation for the immunodominant epitope is fully suppressed. Because of the low accessibility, the total size of the GC response is smaller compared to a GC reaction against the immunodominant epitope. However, the probability of selection of B cells specific for even lower accessible epitopes (3%) is consistently increased by the injection of antibodies (Figure 4C).

The result that the injection of antibodies specific for the immunodominant epitope can shift GC affinity maturation to low-accessible epitopes turned out robust against changing the details of antigen uptake in the model (Figure S3). Affinity-dependent antigen uptake by B cells (Figure S5B) and an impact of antibodies on the amount of accessible antigen on FDC (Figure S5C) turned out indispensable for the shift to low-accessible epitopes. In contrast, the mutation model (Figure S5A), the dynamic control of the number of division (Figure S5E), the spatial GC organization by chemotaxis (Figure S5F), and the exit model (Figures S4 and S6B) as well as the fraction of cells differentiating to output cells upon selection by Tfh (Figures S6C and S6D) modulated the effect of antibody injections only quantitatively, while preserving the qualitative behavior. Tfh polarization to B cells with highest pMHC presentation (Figure S5D) and symmetric versus asymmetric division of B cells (Figures S4 and S6A) hardly changed the result shown in Figure 3. In summary, *in silico* antibody injections can shift GC reactions to focus on low-accessible epitopes and the complex GC simulation allowed the identification of a hierarchy of factors contributing to this shift.

The GC reaction also generates memory B cells. At the time of initiation of a subsequent GC reaction, memory B cells would either differentiate to antibody-forming plasma cells or participate in the GC reaction. The B cell receptors of the memory B cells in the GC face highly competent antibodies stemming from the memory-derived plasma cells, which compete for antigen binding. The model predicts that memory B cells might well participate in GC reactions but will have a competitive disadvantage compared to unrelated naive B cells (Figure 4). Even though both target epitopes are presented at equal frequencies in these simulations, memory B cells are removed from the GC reaction earlier than new B cells unless they managed to survive until they acquired a high number of mutations. The strength of this self-suppression depends on the fraction of memory B cells differentiating to antibody-forming cells (Figure 4). Pre-existing specific antibodies from the primary GC response would further suppress the participation of memory B cells in the secondary response. Thus, antibody feedback provides an additional mechanism of immune memory that allows the progression of antibody responses against various epitopes rather than for them to become trapped in repetitive GC reactions against the same epitope. This mechanism is likely responsible for the occasional natural development of bnAbs.

To test whether this mechanism of self-inhibition can focus a GC reaction onto very-low-accessible epitopes (3%), *in silico* GC founder cells containing 90%, 25%, or 5% memory B cells and variable levels of memory-derived antibody-forming plasma cells were assumed (Figure 4C). The more memory B cells participated in the GC, the less likely the GC responses focused on the low-accessible epitope (Figure 4C). First, because of the lower number of naive B cells, B cells specific for the low-accessible epitope were emerging with even lower frequency, and second, those that developed were rather unlikely to be selected. According to the current belief, secondary GC reactions are dominated by memory-derived founder B cells (Pape et al., 2011). The model predicts an evolutionary advantage of individuals with a higher fraction of re-activated memory B cells that differentiate to antibody-forming plasma cells rather than to GC B cells in the sense that the probability of developing antibodies against low-accessible epitopes is highest without or with only a few memory B cells initiating the GC response.

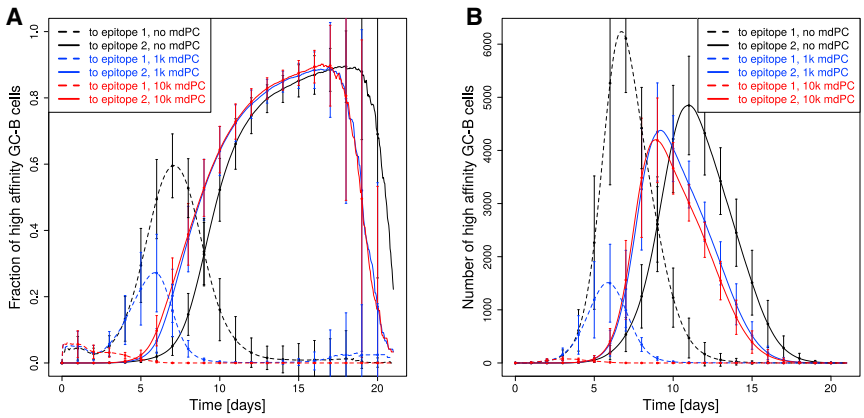

C

setting/readout	Ab-feedback	Ab-injection		memory cells			
number of GCs	960	960	960	960	960	960	960
memory GC founder	0	0	0	90%	25%	5%	5%
mdPC	0	0	0	1000	1000	1000	10000
Ab-injection [nMol]	0	5	50	0	0	0	0
occurred in	**199**	**321**	**248**	**22**	**129**	**200**	**331**
selected in	72	168	136	2	24	58	184
% selected	**36**	**52**	**55**	**9**	**19**	**29**	**56**

Figure 4. Impact of Memory B Cells on Secondary GC Reactions

(A and B) Fraction (A) and number (B) of high-affinity GC-B cells with a dissociation constant of $K_D < 2$ nMol. The simulations start with 5% founder cells from a memory B cell pool specific for epitope 1. Epitope 2 (at a distance of 8 mutations) is presented on FDC with equal frequency. Antibody feedback modulates the binding probability of antigen on FDCs. Antibodies are generated either exclusively by GC output cells (no memory-derived antibody-forming plasma cells [mdPCs]) or, in addition, by mdPCs specific for epitope 1 (with 1,000 [1k] or 10,000 [10k] mdPCs). Note that only high-affinity cells to either of the epitopes are shown, i.e., the GC population is larger. Vertical bars show the standard deviation over 120 simulations for each condition.

(C) *In silico* GC simulations with a ratio of immunodominant to low-accessible epitope of 97:3. Different settings are compared: "Ab-feedback" is the reference simulation in Figure 2 and Figure S2; "Ab-injection" corresponds to Figure 2 and two settings in Figure 3 with injections of different doses of antibodies specific for the immunodominant epitope; "memory cells" assume the presence of memory B cells from a previous GC reaction, where these constitute a fraction of the GC founder cells and contribute to early mdPCs. The number of mdPCs should be interpreted as a strength of antibody production rather than as a number of cells. The readouts comprise the frequency of GCs in which B cells with the highest affinity (dissociation constant K_D, <0.3 nMol) for the low-accessible epitope "occurred in" these would be a result of mutation and are counted irrespective of their fate and their frequency in the GC; the frequency of GCs in which B cells specific for the low-accessible epitope occurred and were "selected in" at least once; and the percentage of GCs classified as selected among those classified as occurred ("% selected"). 960 simulations for each condition.

Interestingly, the presence of antibodies produced by memory-derived antibody-forming cells specific for the 97% immunodominant epitope was able to reduce the frequency of memory B cells participating in the GC response to a similar extent as the injection of antibodies. Memory-derived antibody-forming cells increased both the frequency of occurrence of B cell clones specific for the low-accessible epitope and the probability of their selection (Figure 4C). A minimum number of memory-derived antibody-forming cells was required to achieve the same efficiency as with antibody injections. The required strength of memory-induced self-inhibition is predicted to suppress the participation of memory B cells in GC reactions. This might be tested in experiments in order to decide whether, *in vivo*, this mechanism has the potential to redirect GC responses to other epitopes. It would also be interesting to test strategies of promoting memory B cell differentiation into antibody-forming cells upon reactivation, which, according to the simulations, would strengthen antibody feedback, suppress memory B cell survival in GC reactions, and allow the GCs to focus on so far unappreciated epitopes.

DISCUSSION

It was shown before that increased numbers of Tfh cells might increase the probability of developing bnAbs (De Boer and Perelson, 2017). The present results suggest that it is possible to generate antibodies against low-accessible epitopes when its relative accessibility is increased by antibodies specific for the immunodominant epitopes on FDCs, a mechanism that acts upstream of selection by Tfh cells. Thus, previous results showing that the presence of antibodies can inhibit GC reactions (Zarnitsyna et al., 2016; Zhang et al., 2013) can be turned into a positive effect if the antibodies have the right specificity.

This strategy will have to be tested in experimental settings. Recently, it was found in rhesus macaque monkeys that a slow delivery of HIV envelope trimer antigen was inducing a higher frequency of antibodies directed against non-immunodominant neutralizing epitopes (Cirelli et al., 2019). These data were associated with prolonged GC reactions and affinity maturation. The simulations presented here showed that in normal GC reactions, antibody feedback gets in effect too late for shifting the focus of the reaction to low-accessible epitopes and suggest that persistent GC reactions would not suffer from this limitation. Thus, antibody feedback is a possible explanation of the increased frequency of neutralizing antibodies found in Cirelli et al., (2019), as was also pointed out by the authors.

The simulations predict that memory B cells, which upon reactivation quickly differentiate to generate antibodies, suppress their own participation in the newly mounted GC reaction by antibody feedback. This is in line with the theory of original antigenic sin (Francis, 1960), according to which memory cells would dominate the immune response and prevent adaptation to variations of the pathogen, like in the case of viral drift. In contrast to the theory, the simulation results promote the idea that memory-derived fast antibody responses open the possibility to target other epitopes of the same pathogen in newly mounted GC

reactions with freshly presented antigen, which were not dominant targets of the primary immune response and, thus, are not dominated by memory B cells in the secondary response. In particular, the mechanism of antibody feedback is adaptive in the sense that the participation of memory B cells in GCs is suppressed as long as the affinity of antibodies for the original antigen-epitope is high enough to prevent a selective advantage of memory B cells in the GC. This suggests that GC reactions have evolved to solve new antigenic problems rather than to optimize the already-found solution for old problems.

The impact of antibody feedback onto GC reactions might be further elaborated in the future for vaccination planning. One may consider complementing vaccines with antibody cocktails covering immunodominant epitopes and by this shift the focus of affinity maturation to hardly accessible epitopes that are eventually located in the conserved region of the antigen. It is critical that a wide spectrum of immunodominant epitopes is covered by antibodies, such that the relative accessibility of epitopes in the conserved region is increased. In the context of individualized medicine, this antibody cocktail might be adapted to the individual repertoire of each patient. More generally, the external control of specific antibody generation by injection of antibodies against immunodominant epitopes is worth further exploration.

STAR★METHODS

Detailed methods are provided in the online version of this paper and include the following:

- KEY RESOURCES TABLE
- LEAD CONTACT AND MATERIALS AVAILABILITY
- EXPERIMENTAL MODEL AND SUBJECT DETAILS
- METHOD DETAILS
  - Germinal Centre simulation model
  - Space representation
  - Shape space for antibodies
  - B cell phenotypes
  - Founder cells
  - Antigen-presentation by FDCs
  - Antigen-antibody interaction on FDCs
  - DZ B cell division
  - LZ B cell selection
  - Antibody sources
  - Chemokine distribution
  - Chemotaxis
- QUANTIFICATION AND STATISTICAL ANALYSIS
- DATA AND CODE AVAILABILITY

SUPPLEMENTAL INFORMATION

Supplemental Information can be found online at https://doi.org/10.1016/j.celrep.2019.09.058.

ACKNOWLEDGMENTS

This work was supported by the Human Frontier Science Program (RGP0033/2015) and the Helmholtz Association, Zukunftsthema "Immunology and Inflammation" (ZT-0027). I thank Sebastian Binder for support in R programming for generating the figures from the simulation readout. I thank him and Rebecca Ludwig for revising the manuscript. I thank Sahamoddin Khailaie for generating the graphical abstract.

AUTHOR CONTRIBUTION

M.M.-H. designed the research, developed the simulation software, performed the simulations, evaluated and interpreted the results, and wrote the paper.

DECLARATION OF INTERESTS

The author declares no competing interests.

Received: December 13, 2018
Revised: April 19, 2019
Accepted: September 18, 2019
Published: October 29, 2019

SUPPORTING CITATIONS

The following references appear in the Supplemental Information: Depoil et al. (2005); Meyer-Hermann and Maini (2005).

REFERENCES

Abbott, R.K., Lee, J.H., Menis, S., Skog, P., Rossi, M., Ota, T., Kulp, D.W., Bhullar, D., Kalyuzhniy, O., Havenar-Daughton, C., et al. (2018). Precursor Frequency and Affinity Determine B Cell Competitive Fitness in Germinal Centers, Tested with Germline-Targeting HIV Vaccine Immunogens. Immunity *48*, 133–146.e6.

Allen, C.D., Okada, T., Tang, H.L., and Cyster, J.G. (2007). Imaging of germinal center selection events during affinity maturation. Science *315*, 528–531.

Bache, S.M., and Wickham, H. (2014). magrittr: A Forward-Pipe Operator for R (R package version 1.5.).

Batista, F.D., and Neuberger, M.S. (1998). Affinity dependence of the B cell response to antigen: a threshold, a ceiling, and the importance of off-rate. Immunity *8*, 751–759.

Berek, C., and Milstein, C. (1987). Mutation drift and repertoire shift in the maturation of the immune response. Immunol. Rev. *96*, 23–41.

Binder, S.C., and Meyer-Hermann, M. (2016). Implications of Intravital Imaging of Murine Germinal Centers on the Control of B Cell Selection and Division. Front. Immunol. *7*, 593.

Chaturvedi, A., Martz, R., Dorward, D., Waisberg, M., and Pierce, S.K. (2011). Endocytosed BCRs sequentially regulate MAPK and Akt signaling pathways from intracellular compartments. Nat. Immunol. *12*, 1119–1126.

Cirelli, K.M., Carnathan, D.G., Nogal, B., Martin, J.T., Rodriguez, O.L., Upadhyay, A.A., Enemuo, C.A., Gebru, E.H., Choe, Y., Viviano, F., et al. (2019). Slow delivery immunization enhances HIV neutralizing antibody and germinal center responses via modulation of immunodominance. Cell *177*, 1153–1171.e28.

Corti, D., Cameroni, E., Guarino, B., Kallewaard, N.L., Zhu, Q., and Lanzavecchia, A. (2017). Tackling influenza with broadly neutralizing antibodies. Curr. Opin. Virol. *24*, 60–69.

De Boer, R.J., and Perelson, A.S. (2017). How germinal centers evolve broadly neutralizing antibodies: the breadth of the follicular helper T cell response. J. Virol. *91*, e00983-17.

Depoil, D., Zaru, R., Guiraud, M., Chauveau, A., Harriague, J., Bismuth, G., Utzny, C., Müller, S., and Valitutti, S. (2005). Immunological synapses are versatile structures enabling selective T cell polarization. Immunity *22*, 185–194.

Dustin, M.L., and Meyer-Hermann, M. (2012). Immunology. Antigen feast or famine. Science *335*, 408–409.

Escolano, A., Steichen, J.M., Dosenovic, P., Kulp, D.W., Golijanin, J., Sok, D., Freund, N.T., Gitlin, A.D., Oliveira, T., Araki, T., et al. (2016). Sequential

Immunization Elicits Broadly Neutralizing Anti-HIV-1 Antibodies in Ig Knockin Mice. Cell *166*, 1445–1458.e12.

Figge, M.T., Garin, A., Gunzer, M., Kosco-Vilbois, M., Toellner, K.M., and Meyer-Hermann, M. (2008). Deriving a germinal center lymphocyte migration model from two-photon data. J. Exp. Med. *205*, 3019–3029.

Francis, T. (1960). On the doctrine of original antigenic sin. Proc. Am. Philos. Soc. *104*, 572–578.

Gitlin, A.D., Shulman, Z., and Nussenzweig, M.C. (2014). Clonal selection in the germinal centre by regulated proliferation and hypermutation. Nature *509*, 637–640.

Hannum, L.G., Haberman, A.M., Anderson, S.M., and Shlomchik, M.J. (2000). Germinal center initiation, variable gene region hypermutation, and mutant B cell selection without detectable immune complexes on follicular dendritic cells. J. Exp. Med. *192*, 931–942.

Harrell, F.E., Jr. (2019). Hmisc: Harrell Miscellaneous (R package version 4.2-0).

Hauser, A.E., Junt, T., Mempel, T.R., Sneddon, M.W., Kleinstein, S.H., Henrickson, S.E., von Andrian, U.H., Shlomchik, M.J., and Haberman, A.M. (2007). Definition of germinal-center B cell migration in vivo reveals predominant intrazonal circulation patterns. Immunity *26*, 655–667.

Havenar-Daughton, C., Lee, J.H., and Crotty, S. (2017). Tfh cells and HIV bnAbs, an immunodominance model of the HIV neutralizing antibody generation problem. Immunol. Rev. *275*, 49–61.

Havenar-Daughton, C., Abbott, R.K., Schief, W.R., and Crotty, S. (2018). When designing vaccines, consider the starting material: the human B cell repertoire. Curr. Opin. Immunol. *53*, 209–216.

Helle, F., Duverlie, G., and Dubuisson, J. (2011). The hepatitis C virus glycan shield and evasion of the humoral immune response. Viruses *3*, 1909–1932.

ISO. (2012). ISO/IEC 14882:2011 Information technology—Programming languages—C (International Organization for Standardization).

Kassambara, A. (2018). ggpubr: ggplot2 Based Publication Ready Plots (R package version 0.2).

Kwong, P.D., and Mascola, J.R. (2018). HIV-1 Vaccines Based on Antibody Identification, B Cell Ontogeny, and Epitope Structure. Immunity *48*, 855–871.

Mascola, J.R., and Haynes, B.F. (2013). HIV-1 neutralizing antibodies: understanding nature's pathways. Immunol. Rev. *254*, 225–244.

Meyer-Hermann, M. (2014). Overcoming the dichotomy of quantity and quality in antibody responses. J. Immunol. *193*, 5414–5419.

Meyer-Hermann, M.E., and Maini, P.K. (2005). Cutting edge: back to "one-way" germinal centers. J. Immunol. *174*, 2489–2493.

Meyer-Hermann, M., Deutsch, A., and Or-Guil, M. (2001). Recycling probability and dynamical properties of germinal center reactions. J. Theor. Biol. *210*, 265–285.

Meyer-Hermann, M.E., Maini, P.K., and Iber, D. (2006). An analysis of B cell selection mechanisms in germinal centers. Math. Med. Biol. *23*, 255–277.

Meyer-Hermann, M., Mohr, E., Pelletier, N., Zhang, Y., Victora, G.D., and Toellner, K.M. (2012). A theory of germinal center B cell selection, division, and exit. Cell Rep. *2*, 162–174.

Miller, M.J., Wei, S.H., Parker, I., and Cahalan, M.D. (2002). Two-photon imaging of lymphocyte motility and antigen response in intact lymph node. Science *296*, 1869–1873.

Murira, A., Lapierre, P., and Lamarre, A. (2016). Evolution of the Humoral Response during HCV Infection: Theories on the Origin of Broadly Neutralizing Antibodies and Implications for Vaccine Design. Adv. Immunol. *129*, 55–107.

Nossal, G.J. (1992). The molecular and cellular basis of affinity maturation in the antibody response. Cell *68*, 1–2.

Omori, S.A., Cato, M.H., Anzelon-Mills, A., Puri, K.D., Shapiro-Shelef, M., Calame, K., and Rickert, R.C. (2006). Regulation of class-switch recombination and plasma cell differentiation by phosphatidylinositol 3-kinase signaling. Immunity *25*, 545–557.

Oprea, M., and Perelson, A.S. (1997). Somatic mutation leads to efficient affinity maturation when centrocytes recycle back to centroblasts. J. Immunol. *158*, 5155–5162.

Papa, I., Saliba, D., Ponzoni, M., Bustamante, S., Canete, P.F., Gonzalez-Figueroa, P., McNamara, H.A., Valvo, S., Grimbaldeston, M., Sweet, R.A., et al. (2017). T_{FH}-derived dopamine accelerates productive synapses in germinal centres. Nature *547*, 318–323.

Pape, K.A., Taylor, J.J., Maul, R.W., Gearhart, P.J., and Jenkins, M.K. (2011). Different B cell populations mediate early and late memory during an endogenous immune response. Science *331*, 1203–1207.

Pegu, A., Hessell, A.J., Mascola, J.R., and Haigwood, N.L. (2017). Use of broadly neutralizing antibodies for HIV-1 prevention. Immunol. Rev. *275*, 296–312.

Perelson, A.S., and Oster, G.F. (1979). Theoretical studies of clonal selection: minimal antibody repertoire size and reliability of self-non-self discrimination. J. Theor. Biol. *81*, 645–670.

R Core Team. (2018). R: A language and environment for statistical computing (R Foundation for Statistical Computing).

Randall, T.D., Parkhouse, R.M., and Corley, R.B. (1992). J chain synthesis and secretion of hexameric IgM is differentially regulated by lipopolysaccharide and interleukin 5. Proc. Natl. Acad. Sci. USA *89*, 962–966.

Scheid, J.F., Mouquet, H., Feldhahn, N., Seaman, M.S., Velinzon, K., Pietzsch, J., Ott, R.G., Anthony, R.M., Zebroski, H., Hurley, A., et al. (2009). Broad diversity of neutralizing antibodies isolated from memory B cells in HIV-infected individuals. Nature *458*, 636–640.

Schiffner, T., Sattentau, Q.J., and Dorrell, L. (2013). Development of prophylactic vaccines against HIV-1. Retrovirology *10*, 72.

Schwickert, T.A., Lindquist, R.L., Shakhar, G., Livshits, G., Skokos, D., Kosco-Vilbois, M.H., Dustin, M.L., and Nussenzweig, M.C. (2007). In vivo imaging of germinal centres reveals a dynamic open structure. Nature *446*, 83–87.

Shulman, Z., Gitlin, A.D., Targ, S., Jankovic, M., Pasqual, G., Nussenzweig, M.C., and Victora, G.D. (2013). T follicular helper cell dynamics in germinal centers. Science *341*, 673–677.

Smith, D.J., Lapedes, A.S., de Jong, J.C., Bestebroer, T.M., Rimmelzwaan, G.F., Osterhaus, A.D., and Fouchier, R.A. (2004). Mapping the antigenic and genetic evolution of influenza virus. Science *305*, 371–376.

Thaunat, O., Granja, A.G., Barral, P., Filby, A., Montaner, B., Collinson, L., Martinez-Martin, N., Harwood, N.E., Bruckbauer, A., and Batista, F.D. (2012). Asymmetric segregation of polarized antigen on B cell division shapes presentation capacity. Science *335*, 475–479.

Toellner, K.M., Jenkinson, W.E., Taylor, D.R., Khan, M., Sze, D.M.Y., Sansom, D.M., Vinuesa, C.G., and MacLennan, I.C.M. (2002). Low-level hypermutation in T cell-independent germinal centers compared with high mutation rates associated with T cell-dependent germinal centers. J. Exp. Med. *195*, 383–389.

Tricco, A.C., Chit, A., Soobiah, C., Hallett, D., Meier, G., Chen, M.H., Tashkandi, M., Bauch, C.T., and Loeb, M. (2013). Comparing influenza vaccine efficacy against mismatched and matched strains: a systematic review and meta-analysis. BMC Med. *11*, 153.

Victora, G.D., and Nussenzweig, M.C. (2012). Germinal centers. Annu. Rev. Immunol. *30*, 429–457.

Victora, G.D., Schwickert, T.A., Fooksman, D.R., Kamphorst, A.O., Meyer-Hermann, M., Dustin, M.L., and Nussenzweig, M.C. (2010). Germinal center dynamics revealed by multiphoton microscopy with a photoactivatable fluorescent reporter. Cell *143*, 592–605.

Wang, S., Mata-Fink, J., Kriegsman, B., Hanson, M., Irvine, D.J., Eisen, H.N., Burton, D.R., Wittrup, K.D., Kardar, M., and Chakraborty, A.K. (2015). Manipulating the selection forces during affinity maturation to generate cross-reactive HIV antibodies. Cell *160*, 785–797.

Wang, P., Shih, C.M., Qi, H., and Lan, Y.H. (2016). A Stochastic Model of the Germinal Center Integrating Local Antigen Competition, Individualistic

T-B Interactions, and B Cell Receptor Signaling. J. Immunol. *197*, 1169–1182.

Wickham, H. (2007). Reshaping Data with the reshape Package. J. Stat. Softw. *21*, 1–20.

Wickham, H. (2018). ggplot2: Elegant Graphics for Data Analysis (Springer New York).

Zarnitsyna, V.I., Lavine, J., Ellebedy, A., Ahmed, R., and Antia, R. (2016). Multi-epitope Models Explain How Pre-existing Antibodies Affect the Generation of Broadly Protective Responses to Influenza. PLoS Pathog. *12*, e1005692.

Zhang, Y., Meyer-Hermann, M., George, L.A., Figge, M.T., Khan, M., Goodall, M., Young, S.P., Reynolds, A., Falciani, F., Waisman, A., et al. (2013). Germinal center B cells govern their own fate via antibody feedback. J. Exp. Med. *210*, 457–464.

STAR★METHODS

KEY RESOURCES TABLE

REAGENT or RESOURCE	SOURCE	IDENTIFIER
Software and Algorithms		
C++ ISO/IEC 14882:2011	ISO, 2012	https://www.iso.org/standard/50372.html
R	R Core Team, 2018	https://www.R-project.org/
R package ggplot2	Wickham, 2018	https://ggplot2.tidyverse.org
R package ggpubr	Kassambara, 2018	https://cran.r-project.org/web/packages/ggpubr/index.html
R package Hmisc	Harrell, 2019	https://cran.r-project.org/web/packages/Hmisc/index.html
R package magrittr	Bache and Wickham, 2014	https://cran.r-project.org/web/packages/magrittr/index.html
R package reshape2	Wickham, 2007	https://cran.r-project.org/web/packages/reshape2/index.html

LEAD CONTACT AND MATERIALS AVAILABILITY

Further information and requests can be addressed to Michael Meyer-Hermann (mmh@theoretical-biology.de). This study did not generate new unique reagents.

EXPERIMENTAL MODEL AND SUBJECT DETAILS

This study did not involve any experiments and exclusively relies on computer simulations.

METHOD DETAILS

Germinal Centre simulation model

The GC model assumptions underlying the germinal center (GC) simulations are explained here and include the used parameter values. It follows the description of Meyer-Hermann et al. (2012) adapted to include novel features introduced since then in Meyer-Hermann (2014) and Binder and Meyer-Hermann (2016), as well as the multiepitope representation added here. Used acronyms are: DZ for dark zone, LZ for light zone, Tfh for T follicular helper cell, FDC for follicular dendritic cell.

Space representation

All reactions take place on a three-dimensional discretized space with a rectangular lattice with lattice constant of $\Delta x = 5\ \mu m$. Every lattice node can be occupied by a single cell only.

Shape space for antibodies

Antibodies are represented on a four ($d = 4$) dimensional shape space (Perelson and Oster, 1979). The shape space is restricted to a size of 10 positions per dimension, thus, only considering antibodies with a minimum affinity to the antigen. The optimal clone φ^* is positioned in the center of the shape space. A position on the shape space φ is attributed to each B cell.

The 1-Norm with respect to the optimal clone $\|\varphi - \varphi^*\|_1 = \sum_{i=1}^{d} |\varphi_i - \varphi_i^*|$, i.e., the minimum number of mutations required to reach the optimal clone, is used as a measure for the antigen binding probability. The binding probability is calculated from the Gaussian distribution with width $\Gamma = 2.8$ (Meyer-Hermann et al., 2001):

$$b(\varphi, \varphi^*) = \exp\left(-\frac{\|\varphi - \varphi^*\|_1^2}{\Gamma^2}\right) \quad (1)$$

B cell phenotypes

Three B cell phenotypes are distinguished: DZ B cells, LZ B cells, and output cells. The different phenotypes characterize the cell properties and are not meant as localization within the GC zones. DZ B cells divide, mutate, and migrate. LZ B cells also migrate and undergo the different stages of the selection process. Output cells only migrate.

Founder cells

The model starts from 250 Tfh, 200 FDCs, 300 stromal cells, and no B cell. Tfh are randomly distributed on the lattice and occupy a single node each. Stromal cells are restricted to the DZ (see section Chemokine distribution for their function). FDCs are restricted to the upper half of the reaction sphere, occupy one node by their soma and have 6 dendrites of 40 μm length each. The presence of dendrites is represented as a lattice-node property and, thus, visible to B cells. The dendrites are treated as transparent for B cell or Tfh migration such that they do not inhibit cell motility.

B cell influx rate

As B cell selection is not active during the first 3 days of the reaction (i.e., days 3-5 post immunisation), the first 3 days can be approximated as a B cell expansion phase. Clonality can be safely ignored, and it suffices to consider a single dividing cell type B_i, where i denotes the generation number of the B cells. The dynamics of expansion are then described by

$$\frac{dB_1}{dt} = s - pB_1$$

$$\frac{dB_i}{dt} = 2pB_{i-1} - pB_i \quad \text{for } i > 1 \tag{2}$$

$$\frac{dB_{GC}}{dt} = 2pB_{i_{max}},$$

where s is the influx rate, p the division rate, i_{max} the number of divisions per cell in the expansion phase, and B_{GC} the resulting number of GC B cells that participate in the GC reaction. The number of initial divisions is estimated by the maximum number of divisions observed upon anti-DEC205-OVA treatment, i.e., $i_{max} = 6$ (Victora et al., 2010; Meyer-Hermann et al., 2012). As the division time $\ln(2)/p$ is shorter than the expansion phase $T_{expand} = 3$ days, one may solve Equation (2) in steady state, yielding:

$$B_6 = 2B_5 = 4B_4 = 8B_3 = 16B_2 = 32B_1 = \frac{32s}{p} \tag{3}$$

Thus, the relevant ODE becomes

$$\frac{dB_{GC}}{dt} = 2pB_6 = 64s \overset{yields}{\rightarrow} B_{GC} = 64st \tag{4}$$

i.e., a linear growth in time proportional to the constant influx during expansion. Note that in the steady state approximation the influx rate becomes independent of the division rate p, which is an implication of the assumption of a fixed number of divisions per founder cell i_{max}. With the side condition of getting 9000 cells at day 3, $B_{GC}(T_{expand} = 72\text{hr}) = 9000$, the influx rate is estimated to be

$$s = \frac{B_{GC}(T_{expand})}{64T_{expand}} \approx 2\frac{\text{cells}}{\text{hr}} \tag{5}$$

This corresponds to 144 B cells entering the GC in the first 3 days of expansion and building up the founder cell population of the GC reaction.

Motivated by this estimation, in the model we assumed that B cells enter the GC reaction with a probability corresponding to a rate of 2 cells per hour. New B cells are randomly positioned on the lattice (exclusively on free nodes).

The shape space position of each new B cell is randomly picked from a set of 100 shape space positions at a distance of 5 or 6 mutations to the nearest epitope. Memory-derived founder B cells (see below) are assumed to be optimal clones for a particular epitope, i.e., at distance zero.

Antigen-presentation by FDCs

Each FDC is loaded with 5000 (3000 without antibody feedback) antigen portions distributed onto the lattice nodes occupied by FDC-soma or FDC-dendrite. One antigen portion corresponds to the number of antigen molecules taken up by a B cell upon successful contact with an FDC. For multiple epitopes, both epitopes are presented at each antigen-presenting site with fractions corresponding to their accessibility.

Antigen-antibody interaction on FDCs

Possible sources of antibodies are output cells of the GC reaction, memory-derived antibody-forming plasma cells, and injections (see section Antibody sources below). Antibodies are represented in the 4-dimensional shape space with 10 positions in each direction. The quantity of interest is the amount of free antigen-epitopes at each FDC site when antibodies are present and changing over time. As it is not feasible to calculate the amount of free epitopes at each site for all 10,000 possible antibody types, 11 affinity bins B_{ij} with i element of [0, . . ., 10] were introduced, where the affinity is defined relative to an antigen-epitope j, thus, every epitope gives rise

to its own antibody distribution on affinity bins. We assumed a constant on-rate $k_{on} = 10^6/(\text{Mol sec})$ (Batista and Neuberger, 1998) and a variable off-rate

$$k_{off,i} = \frac{k_{on}}{10^{5.5+0.4i}}, \tag{6}$$

mimicking a dissociation constant that varies over 4 orders of magnitude. At each FDC site x, the chemical kinetics equation for the immune complexes $C_{ij}(x)$ formed between antibodies in bin i and epitopes j

$$\frac{dC_{ij}(x)}{dt} = k_{on}E_j(x)B_{ij} - k_{i,off}C_{ij}(x) \tag{7}$$

was solved for every epitope j in order to determine the amount of free epitope $E_j(x)$ at this site. Only this amount of epitope j is available for B cells to bind antigen with probability according to Equation (1). No additional competitive binding probability as used in Zhang et al. (2013) was assumed here.

DZ B cell division

The average cell cycle duration of 7 h of DZ B cells is varied for each B cell according to a Gaussian distribution. This is needed to get desynchronization of B cell division. The cell cycle is decomposed into four phases (G1, S, G2, M) in order to localize mitotic events if this is needed.

Each founder B cell divides a number of times before differentiating to the LZ phenotype for the first time. Six divisions was the number of divisions found in response to the extreme stimulus with anti-DEC205-OVA (Victora et al., 2010; Meyer-Hermann et al., 2012). Each selected B cell divides a number of times determined by the interaction with Tfh (see below, LZ B cell selection). The parameters of the interaction with Tfh are tuned such that the mean number of divisions is in the range of two (Gitlin et al., 2014). This value is required in order to maintain a DZ to LZ ratio in the range of two (Victora et al., 2010; Meyer-Hermann et al., 2012). A division requires free space on one of the Moore neighbors of the dividing cell. Otherwise the division is postponed until a free Moore neighbor is available.

At every division the encoded antibody can mutate with a probability of 0.5 (Berek and Milstein, 1987; Nossal, 1992). This corresponds to a shift in the shape space to a von Neumann neighbor in a random direction. Upon selection by Tfh the mutation probability is individually reduced from $m_{max} = 0.5$ down to $m_{min} = 0$ in an affinity-dependent way following

$$m(b) = m_{max} - (m_{max} - m_{min})b = \frac{1-b}{2} \tag{8}$$

with b from Equation (1) (Toellner et al., 2002). Thus, after recycling DZ B cells can acquire reduced mutation probabilities. This mechanism is motivated by the observation that B cell receptor internalization enhances the activation of the kinase Akt (Chaturvedi et al., 2011) which, in turn, suppresses activation induced cytosine deaminase (AID) (Omori et al., 2006). AID is required for somatic hypermutation, such that this provides an affinity dependent downregulation of the mutation frequency (Dustin and Meyer-Hermann, 2012). However, there is no formal proof of this mechanism.

B cell division of B cells that previously acquired antigen and have been selected by Tfh distribute the retained antigen asymmetrically to the daughters (Thaunat et al., 2012). The model assumes asymmetric division in 72% of the cases, which is supported by experimental observations (see Thaunat et al., 2012 and Figure S1 in Meyer-Hermann et al., 2012). If division is asymmetric, one daughter gets all the retained antigen while the other gets none, which approximates the value of 88% found in Thaunat et al. (2012). Mutation is suppressed in B cells with retained antigen.

After the required number of divisions, the B cell differentiates with a rate of in 1/6 min to the LZ phenotype. All B cells that kept the antigen up to this time, differentiate to output cells, upregulate CXCR4, and leave the GC in direction of the T zone. The alternatives, that B cells randomly differentiate to output cells after divisions with a probability of 23% (LEDAX model in Meyer-Hermann et al., 2012) or that B cells decide to differentiate to output cells right after interaction with Tfh (BASE mode in Meyer-Hermann et al., 2012), leads to very similar GC readouts (Figure S4 and Figure S6A,B). However, the amount of generated output cells is substantially higher if the B cells differentiate to output cells after divisions as compared to after selection (Dustin and Meyer-Hermann, 2012).

LZ B cell selection

LZ B cells can be in the states unselected, FDC-contact, FDC-selected, Tfh-contact, selected, apoptotic.

Unselected

LZ B cells migrate and search for contact with FDCs loaded with antigen in order to collect antigen for 0.7 h. If an FDC soma or dendrite is present at the position of the B cell, the B cell attempts to establish contact to the epitope with highest affinity to the B cell receptor (default setting). Alternatively, the B cell may attempt to establish contact to the epitope of highest availability at this site (used in Figures S3D–S3F). In both settings, binding is affinity dependent and happens with the probability b in Equation (1). If the available number of antigen portions at the specific FDC site drops below 20 the binding probability b is linearly reduced with the number of available portions. If successful, the B cell switches to the state *FDC-contact*; otherwise the B cell continues

to migrate. Further binding-attempts are prohibited for 1.2 min. At the end of the antigen collection period, B cells switch to the state *FDC-selected*. If a LZ B cell fails to collect any antigen at this time it switches to the state *apoptotic*.

FDC-contact

LZ B cells remain immobile (bound) for 3 min (Schwickert et al., 2007) and then return to the state *unselected*. The counter for the number of successful antigen uptake events is increased by one and the FDC reduces its locally available antigen portions by one.

FDC-selected

B cells search for contact with Tfh. If they meet a Tfh they switch to the state *Tfh-contact*.

Tfh-contact

LZ B cells remain immobile for 6 min. In this time the bound Tfh, which may also be bound to other B cells, polarizes to the bound B cell with highest number of successful antigen uptakes. Only this B cell receives Tfh signals and accumulate those. After the binding time, the B cell detaches and returns to the state *FDC-selected*. It continues to search and bind Tfh cells until the Tfh search time of 3 h is over. Then, it switches to the state *apoptotic* if the accumulated Tfh-signaling time remained below 30 min. Otherwise it switches to the state *selected*.

Selected

LZ B cells keep the LZ phenotype for six hours and desensitize for CXCL13, thus, perform a random walk. During that time they re-enter cell cycle and progress through the cell cycle phases. Then they recycle back to the DZ phenotype with a rate of 1/6 min and memorize the amount of collected antigen as well as the cell cycle phase they have achieved by this time.

The number of divisions $P(A)$ the recycled B cells will do is derived from the amount of collected antigen A, which reflects the amount of pMHC presented to Tfh and the affinity of the B cell receptor for the antigen, as follows:

$$P(A) = P_{\min} + (P_{\max} - P_{\min}) \frac{A^{n_P}}{A^{n_P} + K_P^{n_P}}. \tag{9}$$

The more antigen was collected by the B cell the more divisions are induced. We set the minimum number of division to one ($P_{\min} = 1$) in order to avoid recycling events without further division. It is limited by six divisions in the best case, which is motivated by anti-DEC205-OVA experiments in which DEC205+/+ B cells received abundant antigen which increased pMHC presentation to a maximum (Victora et al., 2010). The population dynamics *in vivo* and *in silico* only matched when the number of divisions was increased to six in the simulation (Meyer-Hermann et al., 2012) suggesting that the strongest possible pMHC presentation to Tfh induces six divisions ($P_{\max} = 6$). The Hill-coefficient was set to $n_P = 2$.

The half value K_P remained to be determined, which denotes the amount of antigen collected by B cells at which the number of divisions becomes half maximal. The number of collected antigen portions varies between zero and a maximum determined by the duration of the antigen collection phase, the duration of each B cell interaction with FDCs, and the migration time between two antigen presenting sites. The numbers of successful B cell-FDC encounters as observed in the simulations served as estimate of $A_{\max}$. Low-affinity B cells had zero or one antigen uptake event, while high-affinity cells took up between 5 and 10 portions. For an intermediate antigen uptake of $A_0 = 4.5$, the resulting number of divisions has to be $P_0 = 2$ in order to be in agreement with the mean number of divisions in the range of two (Gitlin et al., 2014), which leads to the condition:

$$K_P \approx A_0 \left(\frac{P_{\max} - P_{\min}}{P_0 - P_{\min}} - 1 \right)^{1/n_P} = 9. \tag{10}$$

Apoptotic

LZ B cells remain on the lattice for 6 h before they are deleted. They continue to be sensitive to CXCL13 during this time.

Antibody sources

Output cells

Output cells from the GC reaction are collected and memorized together with the affinity of the encoded antibody to the epitopes. Their life time is assumed longer than the duration of the GC reaction. Output cells are attributed to the different affinity bins for each epitope and further differentiate to an antibody forming plasma cell according to a linear rate equation with a rate of ln(2) per day, i.e., with a half life of one day.

All plasma cells produce antibodies B_{ij}, attributed to bin i for each epitope j according to

$$\frac{dB_{ij}}{dt} = \frac{N_{GC} r_Q}{V_{blood}} Q_{ij} - \gamma_B B_{ij}, \tag{11}$$

where $r_Q = 3\ 10^{-18}$mol/hour is the production rate per cell (Randall et al., 1992) and $\gamma_B = \ln(2)/(14\text{days})$ is the degradation rate of antibodies. The produced antibodies are assumed to distribute over the whole organism. The sum of all N_{GC} GC reactions in the organism is diluted over the mouse blood volume V_{blood} and adds up to the total antibody concentration found in the simulated GC. The factor $N_{GC}/V_{blood} = 25$/ml was assumed. This setting implies that antibodies are homogeneously distributed over the space of the simulated GC. Alternative sources of antibodies are plasma cells derived from pre-existing memory B cells from a former GC reaction. Also the injection of antibodies is possible.

Memory-derived plasma cells

Memory-derived plasma cells are assumed to be derived from memory B cells of a previous GC response. In Figure 4, it is assumed that memory B cells specific for the immunodominant epitope pre-exist and contribute to the GC founder cells by 5% of the cells. At the beginning of the GC reaction, these memory B cells are assumed to also quickly differentiate into antibody forming plasma cells. These cells simply add to the number of antibody producing cells Q_{ij} in Equation (11), i.e., $Q_{ij} \rightarrow Q_{ij} + \delta(t)\Delta Q_{ij}$, where $\delta(t)$ is the Dirac-function and $\Delta Q_{ij} = \Delta Q_0$ for a single bin *i* for each epitope *j* and zero otherwise. This means that depending on the encoded antibody type, the produced antibody will be attributed to a different bin *i* for each epitope *j*. The number of memory-derived plasma cells ΔQ_{ij} cannot be interpreted literally, as it represents the product of a potentially different antibody production rate and the actual numbers of cells. Thus, it has to be considered as a scale for the strength of memory-derived antibody production.

Antibody injection

Injection of antibodies is represented by an additional source term $\delta(t - t_{inject})\ \Delta B_{ij}$ in Equation (11) at the particular time point t_{inject}. ΔB_{ij} is $\Delta B_{ij} = \Delta B_0$ for exactly one bin *i* for each epitope *j* and $\Delta B_{ij} = 0$ otherwise. This means that the same amount ΔB_0 is added to every epitope *j*, but to a different affinity bin *I* corresponding to the affinity of the injected antibody to each epitope.

Chemokine distribution

Two chemokines CXCL12 and CXCL13 are considered. CXCL13 is produced by FDCs in the LZ with 10nMol per hour and FDC while CXCL12 is produced by stromal cells in the DZ with 400nMol per hour and stromal cell. As both cell types are assumed to be immobile, chemokine distributions were pre-calculated once and the resulting steady-state distributions were used in all simulations.

Chemotaxis

DZ and LZ B cells regulate their sensitivity to CXCL13 and CXCL12, respectively. This is true in all B cell states unless stated otherwise. All B cells move with a target speed of 7.5 μm/min. This leads to a slightly lower observable average speed of ≈6 μm/min. B cells have a polarity vector that determines their preferential direction of migration. The polarity vector $\vec{p}$ is reset every 1.5 min into a new direction using the chemokine distribution *c* as

$$\vec{p} = \vec{p}_{rand} + \frac{\alpha}{1 + exp\{\kappa(K_{1/2} - \Delta x|\vec{\nabla}c|)\}} \frac{\vec{\nabla}c}{|\vec{\nabla}c|}, \tag{12}$$

where $\vec{p}_{rand}$ is a random polarity vector and the turning angle is sampled from the measured turning angle distribution (Allen et al., 2007; Figure S1B). $\alpha = 10$ determines the relative weight of the chemotaxis and random walk, $K_{1/2} = 2 \cdot 10^{11}$ Mol determines the gradient of half maximum chemotaxis weight, and $\kappa = 10^{10}$/Mol determines the steepness of the weight increase.

B cells de- and re-sensitize for their respective chemokine depending on the local chemokine concentration: The desensitization threshold is set to 6nMol and 0.08nMol for CXCL12 and CXCL13, respectively, which avoids cell clustering in the center of the zones. The resensitization threshold is set at 2/3 and 3/4 of the desensitization threshold for CXCL12 and CXCL13, respectively.

B cells can only migrate if the target node is free. If occupied and the neighbor cell is to migrate in the opposite direction (negative scalar product of the polarity vectors) both cells are exchanged with a probability of 0.5. This exchange algorithm avoids lattice artifacts leading to cell clusters.

Tfh do random walk with a preferential directionality to the LZ: The polarity vector $\vec{p}$ of Tfh is determined from a mixture of random walk $\vec{r}$ and the direction of the LZ $\vec{n}$ by

$$\vec{p} = (1 - \alpha')\vec{r} + \alpha'\vec{n}, \tag{13}$$

where $\alpha' = 0.1$ is the weight of chemotaxis. This weight leads to a dominance of random walk with a tendency to accumulate in the LZ as found in experiment. TCs migrate with an average speed of 10 μm/min and repolarize every 1.7 min (Miller et al., 2002).

Output cell motility is derived from plasma cell motility data to be 3 μm/min (Allen et al., 2007) with a persistence time of 0.75 min.

QUANTIFICATION AND STATISTICAL ANALYSIS

Boxplots in Figures 3, S5, and S6 were generated with R and compared with the Wilcoxon test. Further details can be found in the respective Figure legends.

DATA AND CODE AVAILABILITY

The software used for this study is available at https://gitlab.com/germinalcentres/bnab.